BIOCHEMISTRY
including biophysical chemistry & molecular biology

Article

pubs.acs.org/biochemistry

Utilizing Avidity To Improve Antifreeze Protein Activity: A Type III Antifreeze Protein Trimer Exhibits Increased Thermal Hysteresis Activity

Özge Can[†,‡] and Nolan B. Holland*[,†]

[†]Department of Chemical and Biomedical Engineering, Cleveland State University, 2121 Euclid Avenue, Cleveland, Ohio 44115, United States

[‡]Department of Medical Biochemistry, School of Medicine, Acibadem University, Kayisdagi Cad., No:32, Atasehir, Istanbul, Turkey

ABSTRACT: Antifreeze proteins (AFPs) are ice growth inhibitors that allow the survival of several species living at temperatures colder than the freezing point of their bodily fluids. AFP activity is commonly defined in terms of thermal hysteresis, which is the difference observed for the solution freezing and melting temperatures. Increasing the thermal hysteresis activity of these proteins, particularly at low concentrations, is of great interest because of their wide range of potential applications. In this study, we have designed and expressed one-, two-, and three-domain antifreeze proteins to improve thermal hysteresis activity through increased binding avidity. The three-domain type III AFP yielded significantly greater activity than the one- and two-domain proteins, reaching a thermal hysteresis of >1.6 °C at a concentration of <1 mM. To elucidate the basis of this increase, the data were fit to a multidomain protein adsorption model based on the classical Langmuir isotherm. Fits of the data to the modified isotherms yield values for the equilibrium binding constants for the adsorption of AFP to ice and indicate that protein surface coverage is proportional to thermal hysteresis activity.

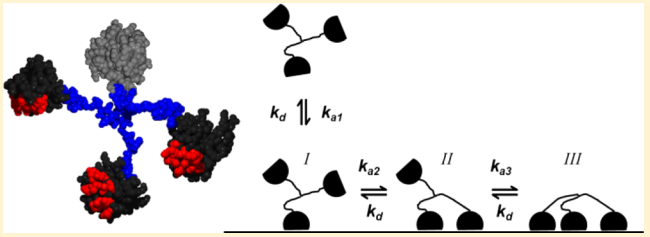

Antifreeze proteins (AFPs) are ice binding proteins found in some plants, insects, and fish that live in extreme environments.[1] These proteins inhibit ice crystal growth and recrystallization[2] and are characterized by thermal hysteresis activity, which is the concentration-dependent difference between the freezing and melting temperatures of protein solutions. AFPs have attracted significant attention because of their potential use in various applications such as frozen food additives, organ/tissue preservation during cold storage, and stabilization of ice slurries for heat transfer.[3−7]

AFPs exhibit thermal hysteresis activity by lowering the freezing point of solutions through irreversible adsorption to ice crystal surfaces and inhibition of ice crystal growth.[8] One model for this concentration-dependent process describes this as a two-step process. (1) At the bulk melting temperature, there is reversible adsorption of AFP at the water−ice interface, and (2) at temperatures below this, the AFP becomes essentially irreversibly bound.[9] This accounts for the observed concentration dependence as well as the observed irreversible adsorption.[10,11]

Analysis of the wide variety of AFPs discovered in numerous organisms has helped to determine what features affect the activity for AFPs.[12−15] The ice binding surface of an AFP typically is planar with amino acid side chains spaced to match an ice crystal lattice.[1,16] It has been observed that comparable AFPs with larger ice binding regions, and therefore greater binding affinity for ice, have greater thermal hysteresis activity. This is principally observed for helical AFPs, in which greater lengths of the AFPs have larger binding areas.[12,13] This concept has been utilized to increase activity by designing proteins with larger binding surfaces. Additional repeats have been added to helical antifreeze proteins, including α-helical type I fish and β-spiral insect AFPs. This has had limited success because there is a diminishing return for each additional turn reportedly because of a reduced level of matching of the ice crystal lattice for added turns.[17]

An alternative mechanism for influencing activity is to have more than one antifreeze protein domain connected together. An increase in the number of binding domains results in an increased avidity of the construct. This is illustrated by RD3, which is a natural two-domain antifreeze protein whose domains are coupled by a flexible linker. Compared to the single-domain analogue, RD3 has increased thermal hysteresis activity at low concentrations while minimally affecting the thermal hysteresis activity at higher concentrations.[18] The conjugation of multiple AFP domains to polymer chains has also been shown to increase thermal hysteresis activity through increased avidity.[19,20] High avidity may also play a role in the hyperactivity of the large type I related antifreeze protein recently discovered.[21]

The increase in thermal hysteresis activity, whether from greater affinity or avidity, is the result of a higher surface

Received: September 30, 2013
Revised: October 31, 2013
Published: November 5, 2013

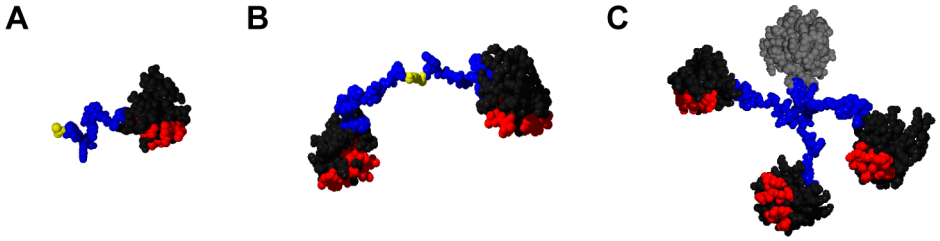

Figure 1. Antifreeze protein constructs. Molecular models of the type III antifreeze proteins as synthesized represent the one-domain (A), two-domain (B), and three-domain (C) proteins. The red residues denote the ice-binding face of the AFP domains. The blue amino acids are parts of the linker, which is terminated either by a cysteine (yellow) or by the foldon domain (gray). The dimer is formed via a disulfide bond of the cysteine residue at the C-terminal linker of the monomer. The trimer is formed by the homotrimerization of the 27-amino acid foldon sequence at the C-terminus. The models were prepared on the basis of the structures of the foldon and the N-terminal domain of RD3 (Protein Data Bank entries 1NAY[26] and 1c8a,[18] respectively), using DeepView/Swiss-PdbViewer.[28]

concentration of AFP at the ice−water interface. Proof of this concept has been elusive because it is experimentally difficult to measure the surface concentration because of the dynamic nature of the system; i.e., the amount of surface area is continually changing because of freezing and/or melting. Even though there have been experimental attempts to determine the surface concentration using fluorescent fusion reporters, the approach was not sufficiently sensitive to be more than qualitative.[10] There have been theoretical predictions of the relationship between surface coverage and thermal hysteresis activity,[22,23] and in a previous report, we developed a model to fit two independent experimental data sets for one- and two-domain proteins that resulted in an empirical relationship between surface coverage and thermal hysteresis activity without assuming any relationship *a priori*.[24] Using a model of two-step protein adsorption based on the classical Langmuir isotherm, we fit data to determine surface coverage, equilibrium constants, and energetics for the adsorption of AFP to ice.[24]

In this work, we expand on our previous report by designing a three-domain AFP using an oligomerization domain, foldon, from bacteriophage T4 fibritin. The foldon sequence, which folds as a stable homotrimer, is added to type III AFP as a fusion domain after a short linker.[25−27] The folded trimer will have three AFP domains that can independently bind to ice, resulting in increased avidity, which is intended to increase the concentration of the surface-bound proteins, particularly at low concentrations. The adsorption model is expanded by adding a third binding step, allowing us to fit thermal hysteresis data of one-, two-, and three-domain AFPs.

MATERIALS AND METHODS

A set consisting of one-, two-, and three-domain type III fish antifreeze proteins was designed on the basis of RD3, a naturally occurring two-domain AFP from the Antarctic eel pout (*Rhigophila dearborni*).[18] Using polymerase chain reaction (PCR), DNA encoding the N-terminal domain and the nine-residue linker of RD3 (RD3N) was amplified from the RD3 gene (generously provided by S. Tsuda, Hokkaido National Industrial Research Institute, Japan). A cysteine residue was added at the C-terminal end of the protein after the linker sequence. Under reducing conditions, this RD3N protein is a single type III AFP domain (Figure 1A). Under nonreducing conditions, cysteines form disulfide bonds resulting in a RD3N dimer [RD3Ndimer (Figure 1B)]. Another modification of RD3N was made, resulting in the formation of a trimer using a foldon domain at the end of a nine-residue linker [RD3Nfoldon (Figure 1C)].

Synthesis and Cloning of the Genes. *Escherichia coli* strain BL21(DE3) (Invitrogen) was used as the cloning and expression host strain. In all experiments, pET20b was used as the plasmid (Novagen). All digestion products were run using agarose gel electrophoresis and column purified.

In the first step of plasmid preparation, the SfiI endonuclease recognition site was created by annealing oligonucleotides 5′-TATGAGCAAAGGGCCGGGCTGGCCGTGAT-3′ and 5′-AATTATCACGGCCAGCCCGGCCCTTTGCTCA-3′ and inserting them into the pET20b vector that had been doubly digested with NdeI and EcoRI endonucleases.

The foldon gene was also produced by annealing the oligonucleotides that were designed to encode the foldon domain and have a SfiI recognition site (5′-TGGCCGGGT-TACATCCCGGAAGCTCCGCGTGACGGTCAGGCTTAC-GTTCGTAAAGACGGTGAATGGGTTCTGCTGTCTACC-TTCCTGTGATAAGGC-3′ and 5′-TTATCACAGGAAGGT-AGACAGCAGAACCCATTCACCGTCTTTACGAACGTA-AGCCTGACCGTCACGCGGAGCTTCCGGGATGTAACC-CGGCCAGCC-3′).

Annealed foldon primers were directly ligated into the pET20b vector that had been singly digested with SfiI. After the single digestion, the DNA was dephosphorylated using Antarctic phosphatase prior to gel purification.

The next step was to add a linker into the vector having a foldon domain and SfiI recognition site. The following linker primers were used in linker annealing: 5′-TGGCCGGACGG-TACCACCTCCAAAGGC-3′ and 5′-TTTGGAGGTGGTAC-CGTCCGGCCAGCC-3′. The annealed linker was then ligated into the SfiI-cut plasmid.

The RD3N gene was amplified from the RD3 gene[18] by PCR using the following primers that introduce 5′ NdeI and 3′ SfiI recognition sites: 5′-TAATACGACTCACTATAGGG-3′ and 5′-CCCAAAGGCCAGCCCGGCCATTCGTAGTTTTT-3′. This amplification produces two bands, one at 595 bp and the other at 295 bp. The lower band was isolated and reamplified using the same primers. This insert was doubly digested with NdeI and SfiI and ligated into the plasmid carrying foldon and linker genes. The resulting amino acid sequence for RD3Nfoldon is MNKASVVANQLIPINTALTLIMMKAEVVT-PMGIPAEEIPNLVGMQVNRAVPLGTTLMPDMVKNYEW-PGWPDGTTSKGWPGYIPEAPRDGQAYVRKDGEWVLLS-TFL.

For the RD3Ndimer construct, the following oligonucleotides were used to produce the linker with a 3′ cysteine: 5′-TATGAGCAAAGGGCCGGGCTGGCCGTGCTGAT-3′ and 5′-AATTATCAGCACGGCCAGCCCGGCCCTTTGCTCA-3′. This annealed oligonucleotide followed by the RD3N gene

dx.doi.org/10.1021/bi401345b | *Biochemistry* 2013, 52, 8745−8752

was added to a pET20b vector with the SfiI recognition sequence as described above to make the RD3N gene with the linker.

Protein Expression. An overnight culture of *E. coli* containing the plasmid of interest in 5 mL of Luria-Bertani (LB) medium was used to inoculate a 1 L culture with 100 μg/mL ampicillin at 37 °C. Protein expression was induced with isopropyl β-D-thiogalactopyranoside (IPTG) after the optical density of the culture had reached a value of 0.6 at 600 nm. The culture was incubated for 6 h at 37 °C. Sodium dodecyl sulfate−polyacrylamide gel electrophoresis (SDS−PAGE) (10 to 20% Tris-glycine) of culture samples that were taken before induction and every hour after induction indicated that the protein was primarily in the insoluble fraction. AFPs were purified using B-PER (Pierce) following the manufacturer's protocol followed by denaturation in 6 M guanidine hydrochloride. Samples were refolded in buffer (50 mM K_2PO_4 and 100 mM NaCl) for 3 days at 4 °C. Each protein was expressed at levels between 50 and 70 mg/L of culture.

Determination of Protein Concentrations. Concentrations of concentrated master solutions of each protein were determined by calculating the molar extinction coefficients by following the procedure given by Gill and von Hippel.[29] This procedure was repeated five times for each protein at each concentration, and a calibration curve was constructed to ensure the linearity of the absorbance values with respect to concentration (data not shown).

Purification and Characterization. A 500 μL aliquot of the sample was loaded onto the 20 mL bioscale size exclusion column filled with Toyopearl HW-55F resin (Tosoh Corp.). The column was filled with the resin according to the manufacturer's instructions. The reaction buffer solution was pumped into the high-performance liquid chromatography (HPLC) column in the down-flow mode at a flow rate of 0.5 mL/min, and UV absorbance values were recorded at 280 nm. Aliquots were collected from the column outlet to be analyzed later. Fractions were concentrated using spin columns (ICON, Pierce) to obtain the master solutions used in thermal hysteresis experiments. The single-domain protein (RD3N) sample was kept under fully reduced conditions in 5 mM tris(2-carboxyethyl)phosphine (TCEP) prior to thermal hysteresis experiments.

The final step of purification for RD3Nfoldon utilized reverse phase HPLC. A gradient of 60% acetonitrile, 30% 2-propanol, and 1% TFA was run on a C18 analytical column (Restek). CD spectra were measured using a circular dichroism spectrometer (Aviv) for the purified RD3Nfoldon sample in the Physiology and Biophysics Department at Case Western Reserve University. The sample was analyzed at 25 °C between 190 and 250 nm.

Thermal Hysteresis Experiments. The interaction of AFPs with ice crystals results in thermal hysteresis, which is the difference between freezing and melting temperatures. Thermal hysteresis activity was measured using a custom-built nanoliter osmometer attached to an optical microscope (Olympus) as previously described.[20,30] Briefly, a single drop of a protein solution was suspended in oil. The droplet was flash-frozen at approximately −40 °C and, after the temperature had been increased to the melting point, thawed slowly (0.01 °C/min) until a single ice crystal was obtained. The temperature at which the crystal began to grow was recorded as the freezing temperature.

Model for Three-Domain Antifreeze Protein Adsorption. For a three-domain protein that allows for independent reversible domain adsorption, there are three different bound conformations, i.e., with one, two, or three domains bound to the surface (Figure 2C). In this model, the fractional surface

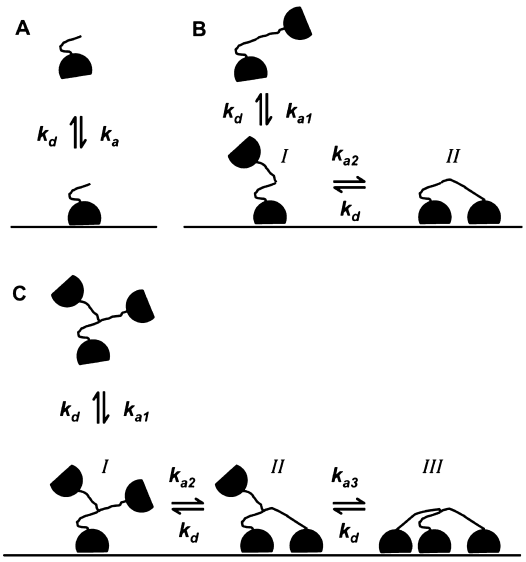

Figure 2. Schematic representation of the adsorption of the different antifreeze proteins to an ice surface. The type III AFP monomer (A) can bind in only one state. The two- and three-domain AFPs can adsorb in multiple states on the surface (B and C, respectively). States I, II, and III represent adsorption with one, two, and three domains adsorbed, respectively. The adsorption rate constants (k_{ai}) will differ, while desorption in all states is governed by a single desorption rate constant, k_d.

coverage, θ, can be described at equilibrium using the rate constants for adsorption and desorption of the individual domains in the manner described previously for the adsorption of a two-domain protein.[24] This modified Langmuir approach assumes monolayer adsorption and that each adsorbed domain occupies an equivalent surface area. When fewer than all three of the domains are bound, the unbound domains can diffuse within the confines of the linker that tethers it to the surface.

When all terms that contribute to formation or elimination of state I are considered, the kinetic equation for state I is

$$\frac{d\theta_1}{dt} = k_{a1}C(1 - \theta_T) - k_d\theta_1 - k_{a2}\theta_1(1 - \theta_T) + k_d\theta_2 \quad (1)$$

where θ_1 and θ_2 are the fractional surface coverage values for state I and state II, respectively. An increase in θ_1 is caused by either adsorption of one domain from the solution with a rate constant of k_{a1} (first term in eq 1) or desorption of one of the domains of a protein with two domains bound to the surface (state II) with a rate constant of k_d (last term in eq 1). Similarly, θ_1 is decreased by desorption of the singly bound domain to the solution with a rate constant of k_d (second term in eq 1) or by adsorption of a second domain to the ice surface with a rate constant of k_{a2} resulting in a state II protein (third term in eq 1). The steps requiring the adsorption of the protein to the surface (first and third terms) are modulated by the fraction of sites that are available for binding, $1 - \theta_T$.

A kinetic equation can similarly be expressed for states II and III:

dx.doi.org/10.1021/bi401345b | *Biochemistry* 2013, 52, 8745−8752

$$\frac{d\theta_2}{dt} = 2k_{a2}\theta_1(1-\theta_T) - 2k_d\theta_2 - 2k_{a3}\theta_2(1-\theta_T) + 2k_d\theta_3 \quad (2)$$

$$\frac{d\theta_3}{dt} = 3k_{a3}\theta_2(1-\theta_T) - 3k_d\theta_3 \quad (3)$$

where k_{a3} is the adsorption rate constant of the third domain, θ_3 is the fractional surface coverage for state III, and $\theta_T = \theta_1 + \theta_2 + \theta_3$. The factors of 2 and 3 arise in eqs 2 and 3, respectively, because protein in state II is 2 times larger and state III has a 3-fold larger surface area than the protein adsorbed in state I.

At equilibrium, eqs 1−3 are equated to zero, and after appropriate substitutions, an algebraic cubic equation for θ_T is obtained, where K_1−K_3 are the equilibrium binding constants (k_{ai}/k_d) for states I−III, respectively:

$$(1-\theta_T)^3 + \frac{1}{K_3}(1-\theta_T)^2 + \frac{1+K_1C}{K_1K_2K_3C}(1-\theta_T) - \frac{1}{K_1K_2K_3C} = 0 \quad (4)$$

The solution for θ_T is given by

$$\theta_T = 1 - \sqrt[3]{-\frac{q}{2} + \sqrt{\frac{q^2}{4} + \frac{p^3}{27}}} - \sqrt[3]{-\frac{q}{2} - \sqrt{\frac{q^2}{4} + \frac{p^3}{27}}} + \frac{a}{3} \quad (5)$$

where

$$q = c + \frac{2a^3 - 9ab}{27} \quad (6)$$

and

$$p = b - \frac{a^2}{3} \quad (7)$$

where a, b, and c are the coefficients of the second, third, and the last terms of eq 4, respectively.

RESULTS

Purification of One- and Two-Domain AFPs. The one- and two-domain AFPs were prepared as a monomer and dimer of the same protein, respectively, the N-terminal domain of RD3 (RD3N). The protein was purified by running the purified RD3N sample through a size exclusion HPLC column under partially reducing conditions (Figure 3).

The first peak in Figure 3 corresponds to the dimer followed by the monomer peak. Approximately two-thirds of the sample formed a dimer as indicated by the relative peak sizes. This method allowed proper separation of the monomer and dimer as indicated by SDS−PAGE, which shows that RD3foldon and RD3Ndimer have been isolated (Figure 4). For this gel, the samples were not boiled prior to injection to retain folding of the foldon domain.

Characterization of the Three-Domain AFP. The three-domain AFP (RD3Nfoldon) results from the trimerization of the protein consisting of RD3N and the 27-amino acid foldon sequence from bacteriophage T4 fibritin connected by a nine-residue linker. To verify the trimerization of purified RD3Nfoldon, Tris-glycine gels were run using purified samples that were heated to different temperatures prior to being loaded.[33] The RD3Nfoldon sample that was injected without heating showed >90% folding comparing the protein band between the 24 and 31 kDa markers (trimer) and the band below the 12 kDa marker (monomer). In the sample that was heated to 50 °C, the trimer:monomer ratio was reduced to approximately 50%, and for the 60 °C sample, nearly all of the trimer was disrupted. For the samples that were heated above 60 °C, only monomer was observed. These results are consistent with the reported instability of the foldon domain at elevated temperatures.[25]

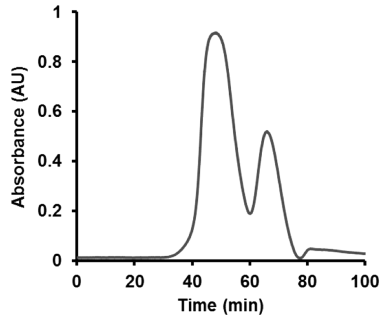

Figure 3. Size exclusion chromatograph of the monomer and dimer type III AFPs. The significantly larger monomer peak has an elution time of 48 min, while the dimer peak has an elution time of 66 min. UV absorbance data were measured at 280 nm.

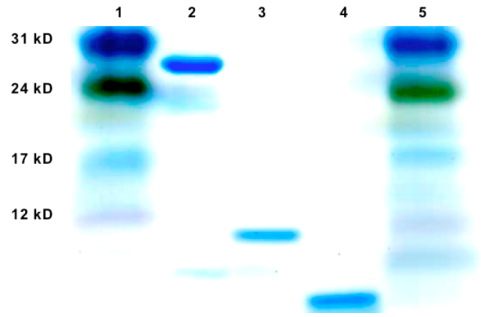

Figure 4. Tris-glycine SDS−PAGE for the three-, two-, and one-domain type III AFPs. Lanes 1 and 5 contained the molecular mass markers. Lane 2 contained RD3Nfoldon (~25 kDa), lane 3 RD3Ndimer (~14 kDa), and lane 4 RD3N (~7 kDa). The one- and two-domain type III AFPs have previously been reported to run slightly faster than their actual molecular masses,[31] while unboiled protein trimers containing an intact foldon have been reported to run slower,[32] which is consistent with these data.

CD spectra for RD3Nfoldon also confirmed the formation of the foldon trimer. The foldon domain, when it is correctly folded, has a fingerprint at 228 nm,[25] and RD3Nfoldon exhibits a pronounced maximum at this wavelength, showing that this protein is correctly folded.

Thermal Hysteresis Activity and Ice Crystal Morphology. The RD3N thermal hysteresis data were consistent with previously reported values.[18] The three-domain RD3Nfoldon showed significantly increased activity compared to that of the one-domain RD3N or the two-domain RD3Ndimer (Figure 5). This increase was more pronounced for the low-concentration region; e.g., the RD3foldon is approximately 10 times as active as the monomer at 150 μM, whereas at 1.5 mM, the activities are different by a factor of ~2.

In the presence of RD3Nfoldon, small (~10 μm) hexagonal bipyramidal ice crystals, characteristic of type III AFPs,[34] formed (Figure 6). The addition of the foldon domain did not affect the ice crystal morphology. This is not unexpected

dx.doi.org/10.1021/bi401345b | Biochemistry 2013, 52, 8745−8752

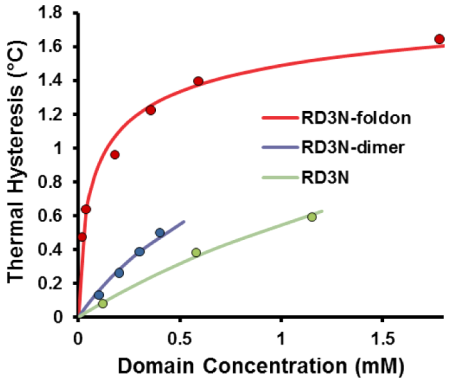

Figure 5. Thermal hysteresis activity for RD3N (green), RD3Ndimer (blue), and RD3Nfoldon (red) as a function of domain concentration measured at a rate of 0.01 °C/min. The data clearly demonstrate that even on a per domain basis the thermal hysteresis activity for the multidomain AFPs is significantly greater at low temperatures.

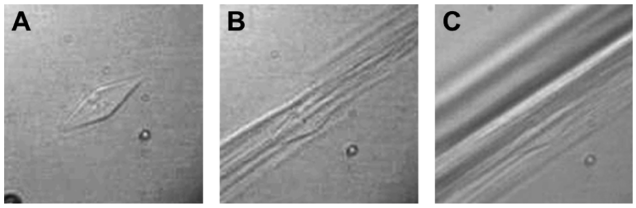

Figure 6. Ice crystal morphologies in the presence of RD3Nfoldon (0.6 mM). Within the thermal hysteresis window, just prior to the burst (or freezing) point (A), the ice crystal is a well-formed hexagonal bipyramid. Immediately after the burst point (B) and shortly after this (C), the crystal is observed to rapidly grow along the *c* axis, which is parallel to the plane of the page.

because the match of the ice biding face of the protein to the ice crystal lattice determines the morphology of the ice crystal. Rapid ice growth along the *c* axis was observed at the freezing point.

Application of the Modified Langmuir Isotherm. Measured thermal hysteresis data were fit to appropriate Langmuir or modified Langmuir equations to determine equilibrium binding constants and to gain insight into the surface coverage necessary to generate thermal hysteresis. The standard Langmuir equation

$$\theta = \frac{KC}{1 + KC} \tag{8}$$

was used for RD3N, and the previously reported Langmuir equation modified for adsorption of a two-domain protein[24]

$$\theta_T = \frac{1}{2K_1K_2}\frac{1}{C} + \frac{1}{2K_2} + 1 - \sqrt{\left(\frac{1}{2K_1K_2}\frac{1}{C} + \frac{1}{2K_2}\right)^2 + \frac{1}{K_1K_2}\frac{1}{C}} \tag{9}$$

was used for RD3Ndimer. Equation 5, as derived above, was used for three-domain RD3Nfoldon.

These three equations relate the surface coverage (θ) to the solution protein concentration (C) through the equilibrium binding constants (K_n). Our measured data are the thermal hysteresis activity as a function of concentration, so a relationship between θ and thermal hysteresis activity needs to be determined to fit our data. Different scaling relationships have been proposed,[22,23] but we do not assume *a priori* any particular scaling relationship between surface coverage and thermal hysteresis activity. We do assume the thermal hysteresis is in some manner dependent on the total surface coverage no matter whether the protein has one, two, or three domains. As will be shown, the three independent data sets allow us to determine the scaling relationship between the total surface coverage and thermal hysteresis activity for this type III AFP. The form of the relationship between the thermal hysteresis activity (TH) and surface coverage is modeled as

$$\mathrm{TH} = A\theta^n \tag{10}$$

where the coefficient A and the exponent n are empirically determined.

This results in eight parameters needed to fit our data: six equilibrium constants total for the three proteins and the coefficient and exponent from eq 10. Recognizing that the various equilibrium constants can be related to each other allows us to reduce the number of fit parameters. As has been the previously described in the development of the two-domain adsorption model,[24] the initial adsorption to the surface can be considered diffusion-limited or adsorption (or collision)-limited. Briefly, the adsorption process can be considered a two-step process: bulk diffusion, which brings the protein close to the ice surface, and binding to the surface. If diffusion is significantly faster than binding, the number of domains that can bind will be important because it will increase the number of collisions leading to an increase in the rate of binding. In this case, the equilibrium binding constant will be proportional to the number of domains available for binding. However, if diffusion is significantly slower than binding, an increased number of domains will not be significant because the binding is not the rate-limiting step. Therefore, the equilibrium binding constant will be independent of domain number. Of course, some intermediate relationship could exist if the rates are comparable, but the values should lie between these two extremes. If we assume a diffusion- or collision-limiting case, the fit is reduced by two degrees of freedom by relating the initial binding constants (K_1) for the three constructs.

When one goes from state I to state II for the two- or three-domain protein, the equilibrium constants are also related. Because the length of the linker that tethers the unbound domains to the surface in each case is the same, it is expected that the equilibrium binding constants for each domain will be the same; however, because the three-domain protein will have two free domains while the two-domain protein will have one domain, the K_2 for RD3Nfoldon will be twice as large as that for RD3Ndimer. This removes one more degree of freedom, leaving five fitting parameters for either the diffusion- or collision-limited case or seven parameters for a free fit without assuming diffusion or collision limiting conditions.

Fits of the data were performed by minimizing the sum squared errors between the measured and calculated thermal hysteresis data as a function of concentration. The seven parameters were calculated using the constraints described above, as well as for diffusion- and collision-limited cases (Table 1). In each case, the data are fit reasonably well, but the collision-limited case resulted in a slightly smaller sum squared error, indicating a better fit. The collision-limited fit was identical to the fit that was done without assuming a diffusion or collision model, but constraining K_1 values to be anywhere between the collision and diffusion conditions (free fit). This supports the idea that the collision relationship is best fit to the

dx.doi.org/10.1021/bi401345b | *Biochemistry* 2013, 52, 8745−8752

Table 1. Fit Parameters for Thermal Hysteresis Data[a]

	free[b]		diffusion[c]	collision[d]	
	TH ∝ θ^n	TH ∝ $\theta^{1/2}$	TH ∝ θ^n	TH ∝ θ^n	TH ∝ θ
RD3N					
K (mM^{-1})	0.38	0.053	0.36	0.38	0.35
RD3Ndimer					
K_1 (mM^{-1})	0.76	0.11	0.36	0.76	0.70
K_2	1.4	0.76	4.0	1.4	1.4
RD3Nfoldon					
K_1 (mM^{-1})	1.1	0.16	0.36	1.1	1.1
K_2	2.8	1.5	8.0	2.8	2.7
K_3	21	27	22	21	21
TH = $A\theta^n$					
A (°C)	2.11	2.26	2.15	2.11	2.11
n	1.04	0.5	1.02	1.04	1.0
rms error ($°C^2$)	0.021	0.038	0.022	0.021	0.021
C_{eff} (mM)	3.7	14.1	11.2	3.7	3.9

[a]Fit constraint: $K_{2,foldon} = 2K_{2,dimer}$. [b]Free: $K \geq K_{1,dimer} \geq 2K$, and $K \geq K_{1,foldon} \geq 3K$. [c]Diffusion: $K = K_{1,dimer} = K_{1,foldon}$. [d]Collision: $K = {}^1/_2K_{1,dimer} = {}^1/_3K_{1,foldon}$.

data. In all three cases, the exponent n, indicating the scaling of TH with surface coverage (θ), is nearly 1. Because a reported model has suggested that TH is proportional to $\theta^{1/2}$,[23] we fit the data with the additional constraint of this relationship. This resulted in a significantly larger root-mean-square (rms) error in the fit as well as a deviation from the shape of the data for the one- and two-domain proteins (Figure 7).

DISCUSSION

Our data clearly demonstrate that the thermal hysteresis activity of an antifreeze protein can be dramatically increased by increasing the number of active AFP domains available for binding. This is particularly evident at low concentrations. Such increased activity has been shown previously by Nishimiya et al., who showed that multimers of type III AFP showed improved thermal hysteresis activity. They produced multimers of RD3N by tandem repetition of these molecules connected by the original nine-residue linker of the naturally occurring two-domain RD3 protein.[35] Their results showed that there was little effect in adding more than two domains. All of the proteins with more than one domain exhibited significantly higher thermal hysteresis activity on a per domain basis than the single-domain protein. However, there was little difference among the two-, three-, and four-domain proteins.[35]

This is in contrast to the results that we observed for the three-domain RD3Nfoldon in this study. As seen for the previously reported two-domain proteins, there is a significant increase in activity of RD3Ndimer versus that of RD3N, but an even greater increase in activity is observed between RD3Ndimer and the three-domain RD3Nfoldon. It was demonstrated with RD3 that the linker is flexible, allowing the two domains to independently bind to the ice surface.[36,37] This is what differentiates the three domains of RD3Nfoldon, which are each free to bind independently, whereas in the tandem repeat structure of Nishimiya et al., the binding of the middle domain(s) is restricted by the two neighboring domains.[35]

On the basis of the fits, the collision-limited adsorption provides the best fit to the data. This is in contrast to the previously reported fit for a dimer and monomer[24] based on the HPLC-12 type III AFP.[38] The fit to the same equations suggested that the fit was better fit by diffusion-limited adsorption. This may be because the binding affinity of HPLC-12 is significantly greater than that of RD3N as indicated by their equilibrium binding constants, 1.9 and 0.38 mM^{-1}, respectively. Because of the weaker binding of RD3N, it requires a relatively larger number of collisions to result in a binding event, pushing it toward a collision-limited process. It is notable that even though the RD3N monomer has significantly weaker binding than HPLC-12, RD3Nfoldon exhibits greater thermal hysteresis activity than the dimer of HPLC-12, indicating the benefit of the additional domain.

The fit of our data suggests a proportional relationship between surface coverage and thermal hysteresis activity. The proposed relationship that thermal hysteresis activity is proportional to the square root of surface coverage[23] does not satisfactorily fit our data. The previously reported fit to HPLC-12 also resulted in a similar linear relationship between surface coverage and thermal hysteresis activity.[24] Extrapolation of the linear relationship to full surface coverage gives a limit of thermal hysteresis activity for a given AFP domain. In the case of RD3N, the limit is 2.1 °C. As the data reach a surface coverage of only 0.75, it is possible that this relationship breaks down at higher surface coverages.

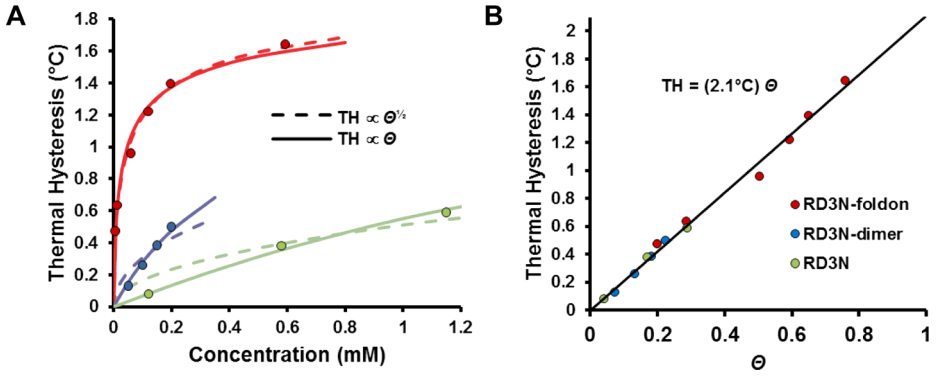

Figure 7. (A) Fits of thermal hysteresis data for RD3N (green), RD3Ndimer (blue), and RD3Nfoldon (red) as a function of protein concentration. The solid lines represent fits of the data where the thermal hysteresis activity is proportional to surface coverage (θ). The dashed line is a fit based on the thermal hysteresis activity being proportional to $\theta^{1/2}$. (B) Thermal hysteresis activity as a function of surface coverage based on the collision-limited model. This illustrates the linear relationship between thermal hysteresis activity and surface coverage.

dx.doi.org/10.1021/bi401345b | Biochemistry 2013, 52, 8745−8752

The equilibrium binding constant for the third domain of RD3Nfoldon, as fit to the data, is nearly 1 order of magnitude larger compared to the binding constant of the second domain. This would not be expected if the unbound domain were completely free to diffuse at the end of its linker; however, it could occur if the domain were forced into an orientation that promotes its binding to the surface. This is possible because the three linkers come out one direction from the foldon domain, so once two domains are bound, the third is directed to the surface. When there are two free domains, the domains have greater freedom of motion. The increased level of binding of the third domain leads to a higher surface coverage than what would occur if the third domain were not oriented, directly contributing to the enhanced activity.

The successful fit of our data by the Langmuir and modified Langmuir models suggests that these models are adequate for describing the behavior of the system. Although other approaches such as statistical thermodynamics may provide a slightly more accurate fit to the data,[39] they would not significantly impact the essence of our results.

CONCLUSIONS

We have successfully expressed and characterized type III AFP constructs to increase thermal hysteresis activity. Foldon, an oligomerization domain, was used to create a type III AFP trimer that is more active than the one-domain type III AFP, yielding a 1.65 °C thermal hysteresis activity at 0.6 mM. In addition, we have developed a new model to describe three-domain protein adsorption based on the classical Langmuir model. Using classical and modified Langmuir models, the relationship between surface coverage and thermal hysteresis activity and equilibrium binding constants were obtained for a type III antifreeze protein. It should be noted that modified Langmuir isotherms derived in this study can be of general use and can be further modified and extended to other molecular constructs with more than three independent binding regions.

The increased activity is attributed to avidity, which increases activity at low concentrations but does not increase the maximal theoretical thermal hysteresis activity. To accomplish this, the oligomerization approach could be extended to hyperactive insect AFPs to increase the maximal thermal hysteresis activity. Nevertheless, designing AFP constructs that have higher thermal hysteresis activities at significantly lower concentrations would make it much more economical to use them as cryopreservation additives and ice slurry stabilizers.

AUTHOR INFORMATION

Corresponding Author

*E-mail: n.holland1@csuohio.edu. Phone: (216) 687-2572.

Funding

This research was supported by the American Heart Association (Scientist Development Grant 0635084N) and the Cleveland State University Doctoral Dissertation Research Expense Award Program.

Notes

The authors declare no competing financial interest.

ACKNOWLEDGMENTS

We thank A. H. Heuer and A. McIlwain (Case Western Reserve University) for the use of and assistance with the nanoliter osmometer.

REFERENCES

(1) Jia, Z. C., and Davies, P. L. (2002) Antifreeze proteins: An unusual receptor-ligand interaction. *Trends Biochem. Sci. 27*, 101−106.
(2) Young, H. M., and Fletcher, G. L. (2008) Antifreeze protein gene expression in winter flounder pre-hatch embryos: Implications for cryopreservation. *Cryobiology 57*, 84−90.
(3) Chao, H. M., Davies, P. L., and Carpenter, J. F. (1996) Effects of antifreeze proteins on red blood cell survival during cryopreservation. *J. Exp. Biol. 199*, 2071−2076.
(4) Amir, G., Rubinsky, B., Kassif, Y., Horowitz, L., Smolinsky, A. K., and Lavee, J. (2003) Preservation of myocyte structure and mitochondrial integrity in subzero cryopreservation of mammalian hearts for transplantation using antifreeze proteins: An electron microscopy study. *European Journal of Cardio-Thoracic Surgery 24*, 292−297.
(5) Soltys, K. A., Batta, A. K., and Koneru, B. (2001) Successful nonfreezing, subzero preservation of rat liver with 2,3-butanediol and type I antifreeze protein. *J. Surg. Res. 96*, 30−34.
(6) Inada, T., and Modak, P. R. (2006) Growth control of ice crystals by poly(vinyl alcohol) and antifreeze protein in ice slurries. *Chem. Eng. Sci. 61*, 3149−3158.
(7) Egolf, P. W., and Kauffeld, M. (2005) From physical properties of ice slurries to industrial ice slurry applications. *Int. J. Refrig. 28*, 4−12.
(8) Knight, C. A., Cheng, C. C., and Devries, A. L. (1991) Adsorption of α-helical antifreeze peptides on specific ice crystal-surface planes. *Biophys. J. 59*, 409−418.
(9) Kristiansen, E., and Zachariassen, K. E. (2005) The mechanism by which fish antifreeze proteins cause thermal hysteresis. *Cryobiology 51*, 262−280.
(10) Pertaya, N., Marshall, C. B., DiPrinzio, C. L., Wilen, L., Thomson, E. S., Wettlaufer, J. S., Davies, P. L., and Braslavsky, I. (2007) Fluorescence microscopy evidence for quasi-permanent attachment of antifreeze proteins to ice surfaces. *Biophys. J. 92*, 3663−3673.
(11) Celik, Y., Drori, R., Pertaya-Braun, N., Altan, A., Barton, T., Bar-Dolev, M., Groisman, A., Davies, P. L., and Braslavsky, I. (2013) Microfluidic experiments reveal that antifreeze proteins bound to ice crystals suffice to prevent their growth. *Proc. Natl. Acad. Sci. U.S.A. 110*, 1309−1314.
(12) Chao, H., Hodges, R. S., Kay, C. M., Gauthier, S. Y., and Davies, P. L. (1996) A natural variant of type I antifreeze protein with four ice-binding repeats is a particularly potent antifreeze. *Protein Sci. 5*, 1150−1156.
(13) Leinala, E. K., Davies, P. L., Doucet, D., Tyshenko, M. G., Walker, V. K., and Jia, Z. C. (2002) A β-helical antifreeze protein isoform with increased activity: Structural and functional insights. *J. Biol. Chem. 277*, 33349−33352.
(14) Gauthier, S. Y., Marshall, C. B., Fletcher, G. L., and Davies, P. L. (2005) Hyperactive antifreeze protein in flounder species. *FEBS J. 272*, 4439−4449.
(15) Marshall, C. B., Chakrabartty, A., and Davies, P. L. (2005) Hyperactive antifreeze protein from winter flounder is a very long rod-like dimer of α-helices. *J. Biol. Chem. 280*, 17920−17929.
(16) Sonnichsen, F. D., Sykes, B. D., Chao, H., and Davies, P. L. (1993) The nonhelical structure of antifreeze protein type-III. *Science 259*, 1154−1157.
(17) Marshall, C. B., Daley, M. E., Sykes, B. D., and Davies, P. L. (2004) Enhancing the activity of a β-helical antifreeze protein by the engineered addition of coils. *Biochemistry 43*, 11637−11646.
(18) Miura, K., Ohgiya, S., Hoshino, T., Nemoto, N., Suetake, T., Miura, A., Spyracopoulos, L., Kondo, H., and Tsuda, S. (2001) NMR analysis of type III antifreeze protein intramolecular dimer: Structural basis for enhanced activity. *J. Biol. Chem. 276*, 1304−1310.
(19) Esser-Kahn, A. P., Trang, V., and Francis, M. B. (2010) Incorporation of antifreeze proteins into polymer coatings using site-selective bioconjugation. *J. Am. Chem. Soc. 132*, 13264−13269.
(20) Can, O., and Holland, N. B. (2011) Conjugation of type I antifreeze protein to polyallylamine increases thermal hysteresis activity. *Bioconjugate Chem. 22*, 2166−2171.

(21) Graham, L. A., Marshall, C. B., Lin, F. H., Campbell, R. L., and Davies, P. L. (2008) Hyperactive antifreeze protein from fish contains multiple ice-binding sites. *Biochemistry 47*, 2051−2063.
(22) Burcham, T. S., Osuga, D. T., Yeh, Y., and Feeney, R. E. (1986) A kinetic description of antifreeze glycoprotein activity. *J. Biol. Chem. 261*, 6390−6397.
(23) Wang, S., Amornwittawat, N., and Wen, X. (2012) Thermodynamic analysis of thermal hysteresis: Mechanistic insights into biological antifreezes. *J. Chem. Thermodyn. 53*, 125−130.
(24) Can, O., and Holland, N. B. (2009) Modified Langmuir isotherm for a two-domain adsorbate: Derivation and application to antifreeze proteins. *J. Colloid Interface Sci. 329*, 24−30.
(25) Frank, S., Kammerer, R. A., Mechling, D., Schulthess, T., Landwehr, R., Bann, J., Guo, Y., Lustig, A., Bachinger, H. P., and Engel, J. (2001) Stabilization of short collagen-like triple helices by protein engineering. *J. Mol. Biol. 308*, 1081−1089.
(26) Stetefeld, J., Frank, S., Jenny, M., Schulthess, T., Kammerer, R. A., Boudko, S., Landwehr, R., Okuyama, K., and Engel, J. (2003) Collagen stabilization at atomic level: Crystal structure of designed (GlyProPro)(10)foldon. *Structure 11*, 339−346.
(27) Ghoorchian, A., Vandemark, K., Freeman, K., Kambow, S., Holland, N. B., and Streletzky, K. A. (2013) Size and shape characterization of thermoreversible micelles of three-armed star elastin-like polypeptides. *J. Phys. Chem. B 117*, 8865−8874.
(28) Guex, N., and Peitsch, M. C. (1997) SWISS-MODEL and the Swiss-PdbViewer: An environment for comparative protein modeling. *Electrophoresis 18*, 2714−2723.
(29) Gill, S. C., and von Hippel, P. H. (1989) Calculation of protein extinction coefficients from amino-acid sequence data. *Anal. Biochem. 182*, 319−326.
(30) Chakrabartty, A., and Hew, C. L. (1991) The effect of enhanced α-helicity on the activity of a winter flounder antifreeze polypeptide. *Eur. J. Biochem. 202*, 1057−1063.
(31) Wang, X., DeVries, A. L., and Cheng, C. C. (1995) Antifreeze peptide heterogeneity in an antarctic eel pout includes an unusually large major variant comprised of two 7 kDa type III AFPs linked in tandem. *Biochim. Biophys. Acta 1247*, 163−172.
(32) Ghoorchian, A., and Holland, N. B. (2011) Molecular architecture influences the thermally induced aggregation behavior of elastin-like polypeptides. *Biomacromolecules 12*, 4022−4029.
(33) Ghoorchian, A., Cole, J. T., and Holland, N. B. (2010) Thermoreversible micelle formation using a three-armed star elastin-like polypeptide. *Macromolecules 43*, 4340−4345.
(34) Davies, P. L., Baardsnes, J., Kuiper, M. J., and Walker, V. K. (2002) Structure and function of antifreeze proteins. *Philos. Trans. R. Soc., B 357*, 927−933.
(35) Nishimiya, Y., Ohgiya, S., and Tsuda, S. (2003) Artificial multimers of the type III antifreeze protein: Effects on thermal hysteresis and ice crystal morphology. *J. Biol. Chem. 278*, 32307−32312.
(36) Holland, N. B., Nishimiya, Y., Tsuda, S., and Sonnichsen, F. D. (2007) Activity of a two-domain antifreeze protein is not dependent on linker sequence. *Biophys. J. 92*, 541−546.
(37) Holland, N. B., Nishimiya, Y., Tsuda, S., and Sönnichsen, F. D. (2008) Two domains of RD3 antifreeze protein diffuse independently. *Biochemistry 47*, 5935−5941.
(38) Baardsnes, J., Kuiper, M. J., and Davies, P. L. (2003) Antifreeze protein dimer: When two ice-binding faces are better than one. *J. Biol. Chem. 278*, 38942−38947.
(39) Quiroga, E., and Ramirez-Pastor, A. J. (2013) Statistical thermodynamics of molecules with multiple adsorption states: Application to protein adsorption. *Chem. Phys. Lett. 556*, 330−335.